Submitted to ADVANCED MATERIALS
DOI: 10.1002/adma.((please add manuscript number))

**Etching Diamond Nanostructures: A masking mechanism**

By *W.R. McKenzie*, and P.R. Munroe*

[*] Electron Microscope Unit, Mark Wainwright Analytical Centre
Basement, Chemical Sciences Building
The University of New South Wales
NSW 2052
AUSTRALIA

E-mail: Warren.McKenzie@unsw.edu.au

Keywords: hard mask, focussed ion beam, diamond, lithography, TEM

Diamond is a unique material being biocompatible, chemically inert, a high mobility semiconductor, and one which intrinsically possesses a number of extreme material properties such as the highest Young's modulus, hardness, thermal conductivity, number density of atoms and widest optical bandgap.[1,2] The past decade has seen a number of developments in the fabrication of diamond, which has enabled its functionalisation. These have led to the rapid evolution a number of practical applications in the areas of optoelectronics,[3] photonics,[1-2, 4] micro/nanoelectronic,[5] micro-electro-mechanical systems (MEMS),[6] atomic force microscopy (AFM),[7] biomedical devices,[8] field emission (e.g. flat panel displays),[9-10] nano-imprint lithography (for the patterning of integrated circuits),[11] and electrochemical bio-sensors detecting glucose [12] and DNA.[13-15] Generally, such applications require a lithographic surface patterning step for their functionalisation.

Typically, lithographic patterning of diamond involves resist-based processing to deposit a patterned hard mask, for example silicon[16-17] or aluminium,[11] against an oxygen-containing plasma or reactive ion etch. Once oxidized by the plasma this layer is resistant to the reactive component of the etch, which is primarily responsible for removing the un-masked diamond, since it etches at a slower rate.

The Focused Ion Beam Hard Mask (FIBHM) recently developed by McKenzie et al. (2009) [18-19] represents a significant leap forward in the ability to pattern nano-scaled structures on to diamond surfaces as it is a direct-write process and does not involve the deposition of a resist or any other sacrificial layer. This distinction brings many advantages of the FIBHM over traditional means of lithographic patterning and, thus, it is expected to find many applications where diamond is a candidate material for new technologies.

Application of the FIBHM has already demonstrated improvements relative to existing conventional surface patterning techniques. For example, in the preparation of nano-imprint and imprint lithography dies where 100nm structures patterned onto the tip have been replicated via imprint into silicon.[19] A second application is for the fabrication of photonic waveguides structures,[20] where sidewall roughness values were measured to be $< 1$nm RMS,[19] an improvement from ~20nm obtained using traditional techniques.[16, 21] These improvements are expected to allow miniturisation to occur as smoother sidewalls reduce light scattering along the length of the waveguide.

The FIBHM has been predicted to outperform resist-based lithography for ultimate feature resolution.[18] To date, patterned line widths of 25nm have been achieved, a significant improvement on 100nm for diamond using other masking techniques patterned with electron beam lithography.[21] It is reasonably expected that sub-10nm resolutions are achievable if modern ion optics are used (currently ~ 2.5nm) which would likely have a very significant impact on the lithography field where ultimate resolution of patterned features is limited to ~10nm depicted by the chain length of polymer resists.[22]

Despite the recent interest in the FIBHM, the underlying masking mechanism has not been previously reported. However, it has been shown that the FIBHM was effective against an Ar-based (inert) plasma,[20] which indicated the mechanism is fundamentally different to other hard masks used for diamond, which rely on a reactive component of the plasma etch.

We present an analytical scanning electron microscope (SEM) and transmission electron microscope (TEM) study of the FIBHM process. Plasma etched diamond reveals a layer incidentally deposited as an artifact of this process which is shown to grow in areas where the focused ion beam (FIB) has implanted gallium. Based on these findings we propose a novel masking mechanism as a new form of ion beam lithography, demonstrate this masking mechanism explains the formation of diamond nano-whisker structures similar to those used for diamond-based sensors,[13-15] and predict that the masking mechanism will be useful for other substrates, such as silicon.

The FIBHM process is illustrated in **Fig. 1**. It involves a two stage process, where, Step 1 exposes the surface to a light dose of $Ga^+$ ions (>$7.5\times10^{15}$ $cm^{-2}$) from a FIB system, which locally modifies the surface creating a mask against a plasma etch. Subsequently, Step 2 employs a plasma etch (e.g. oxygen or argon) to reveal the patterned structures by etching the surrounding material.

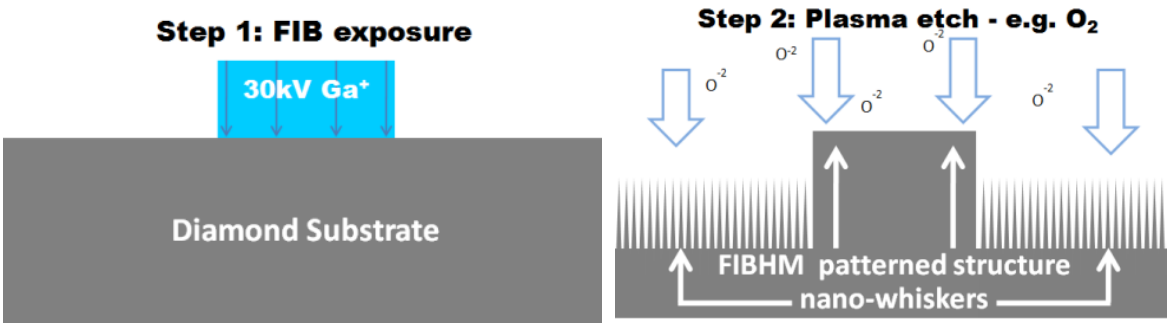

Fig. 1: The Focused Ion Beam Hard Mask technique: Step 1 is a local exposure of the diamond surface with a $Ga^+$ Focused Ion Beam microscope. Step 2 is a plasma etch of the diamond leaving the patterned areas raised as they have been masked from the etch by the FIBHM. Nano-whiskers can form around the un-exposed areas as indicated.

The microstructure following the FIB exposure into diamond, equivalent to Step 1, has recently been studied by McKenzie et al. (2010).[23] The FIB implantation, at an energy of 30kV and dose above $10^{16}$ $Ga^+/cm^2$, creates an amorphous carbon layer ~37nm deep which contains a significant concentration of gallium and whose outer surface is a gallium oxide containing very little carbon.

Results from TEM and SEM analysis of the masking layer and structures created following Step 2 of the FIBHM with an oxygen plasma etch are shown in **Fig. 2**. Fig. 2(A) is a secondary electron image of a solid structure created using a FIBHM, as well as nano-whiskers formed in the surrounding etched region. Fig. 2(B) shows a bright field TEM cross-sectional image of a similarly patterned structure (also showing nano-whiskers) indicating the a-C + Ga layer, which appears to be similar to the as-implanted gallium reported in literature.[23] The resilience of this layer to the etching step demonstrates its effect as a mask against an oxygen plasma. The inset in this image (white rectangular outline) is shown at a higher magnification in Fig. 2(C). It highlights the gallium containing amorphous carbon product of the Step 1 (FIB implantation) below an additional layer ~10nm thick. An energy dispersive X-ray (EDX) analysis of this layer in Fig. 2(D) reveals significant compositions of Fe, O, C and Ga. Based on the surface composition of as FIB- implanted diamond reported in the literature[23] O, C and Ga are expected in this layer, however the presence of Fe is not.

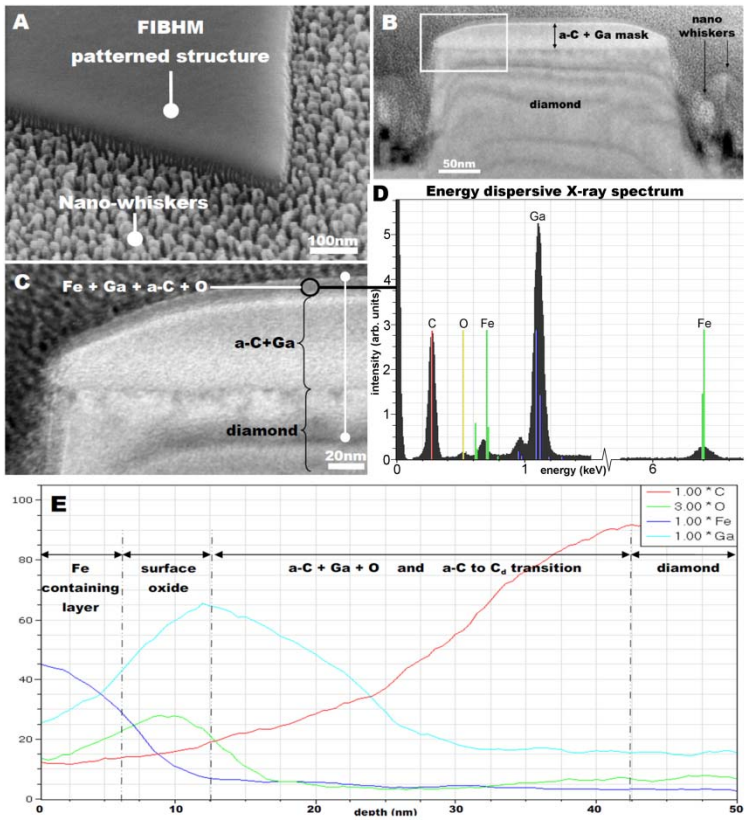


Fig. 2: Evidence of a novel mechanism for the masking of diamond from a plasma etch. (A) Secondary electron image of a solid structure created using the FIBHM technique, taken with the stage tilted 52º from the plan view of the film. (B) bright field TEM image of a patterned structure cross-section created with the FIBHM showing the mask layer of amorphous carbon and gallium (a-C + Ga) and diamond nano-whiskers outside the area defined for the pattern. (C) Bright field TEM of the inset in B (white rectangular outline) highlighting the positions of the diamond, a-C+Ga layer from the Ga-implantation, and additional layer containing Fe from the oxygen plasma etch step. (D) EDX spectrum from the Fe-rich layer defined in (C) indicating the presence of Fe, O and C. (E) TEM EDX line scan, over the white indicator line in (C).

Fig. 2 (E) shows an EDX line scan from across the a-C + Ga layer after it has been exposed to an oxygen plasma etch. The equivalent position of this line scan is shown by the white indicator line shown in Fig. 2(C). The layers described as “surface oxide” and “a-C + Ga + O” through to the diamond closely correspond to the profile of as $Ga^+$ FIB implanted diamond reported in literature[23] and are believed to be unchanged by the plasma treatment.

Fig. 2(E) shows the position of this Fe-containing layer above the "surface oxide", which indicates that the plasma etch has not significantly affected this layer, with the exception of the addition of this Fe-containing material. Supported by observations of a similar Fe-containing deposition arising from an etch facility[24], we believe that source of the iron is from the plasma sputtering atoms from components in the stainless steel vacuum chamber of the plasma etch system. These ultimately re-deposit on the "a-C+Ga+O" surface which, being an oxide inherently have a high affinity for metals relative to the diamond surface.

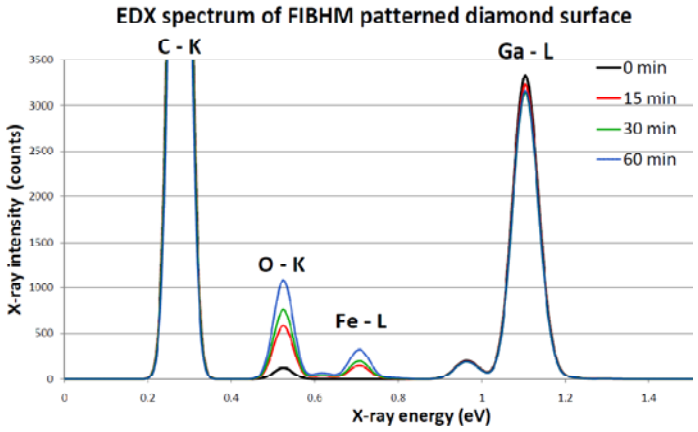


Fig. 3: EDX spectrum from FIBHM masked areas for various plasma etch times. An incident scanning electron beam of 3keV was used to obtain a shallow sampling of the X-rays in order to detect the Fe layer in the outer few nanometers of the surface. C-K, O-K, Fe-L and Ga-L peaks are indicated. Results show that counts from Fe and O increase with increased plasma exposure time, while the Ga peak appears to be unchanged. These results suggest that the gallium-rich layer (a-C+Ga) is not being etched by the plasma whilst the outer surface layer containing Fe and O is expanding.

The iron-containing oxide layer was studied as a function of oxygen plasma etch time using a low energy EDX analysis. Results are shown in **Fig. 3** and demonstrate that the Fe-containing oxide layer is expanding during etching. The as-implanted sample "0 min" shows the surface

composition including significant C, O and Ga which agree with the EDX results in Fig. 1. Applying the oxygen plasma for 15, 30 and 60 minutes, the Fe-peak grows in intensity with the oxygen peak. This increase in intensity is believed to be due to the Fe and O containing layer increasing in thickness representing a greater proportion of the EDX sampling volume. The gallium peak is relatively unchanged in comparison suggesting that the a-C layer housing the gallium (a-C+Ga) is not being consumed. Thus, it appears that on exposure to the plasma the Fe-containing layer is an oxide which is growing and protects the underlying a-C+Ga layer ultimately preventing any oxygen interactions with the underlying diamond masking it against the plasma etch.

A $Ga^+$ FIB exposure of diamond display a unique interaction that produces a carbonatious layer that holds a significant concentration of gallium (and oxygen) in its surface[23] (Step 1 of the FIBHM). During a plasma exposure which etches the naked diamond (Step 2 of the FIBHM) this FIB-exposed surface captures Fe, which occurs as an impurity generated as an artifact of the plasma generation process, and deposits this element in the form of a thin Fe-containing oxide layer. This layer is observed above the "surface oxide" layer incidental to the FIB implantation and is seen to grow as a function of etch time, as described in Fig. 3. This layer is thicker than the implantation depth of the ions accelerated towards the surface by the DC bias in the plasma etcher (<1nm, based on TRIM calculations), thus this self-grown layer isolates both the "a-G + Ga" layer and underlying diamond from the plasma etch producing an effective self-grown hard mask.

This masking behavior is fundamentally different to any other phenomena described in literature for surface patterning, since it combines the deposition of the effective masking layer and etch in the same plasma exposure step. Thus, we propose a novel masking mechanism underpinning the Focused Ion Beam Hard mask as: a surface modification (e.g.

via a FIB implantation from step 1 of the FIBHM) which leads to the formation of a non-volatile platform (e.g. the a-C+Ga+O layer) on which components in the plasma can deposit (e.g. Fe and O) that subsequently protect the underlying or unmasked material (e.g. diamond) from etching in the same plasma environment.

We believe the most critical elements for the mask are that the modified surface layer is stable under the plasma (relative to the unmodified substrate) and the components in the plasma have a high affinity for this surface layer to allow such a deposition in an otherwise erosive environment. Two situations which we believe meet this condition are discussed: $Ga^+$ FIB implanted silicon, and impurities in diamond which lead to the formation of nano-whisker structures.

A number of studies[25-27] have reported $Ga^+$ FIB-exposed silicon to be resistant to a plasma etch containing oxygen and $SF_6$, however none have conclusively reported the masking mechanism. Relative etch rates between the Ga-implanted to non-implanted surface of at least 1000:1 were demonstrated and used to create pillar-type structures.[26] Secondary ion mass spectrometry measurements of the outer surface of $Ga^+$ FIB-implanted silicon[27] reveal that, like $Ga^+$ FIB-implanted diamond, the outer surface is predominantly a gallium oxide containing little substrate material. Given that the same surface condition which leads to deposition of the Fe-containing layer in the diamond case would be met for FIB-implanted silicon we predict the mechanism proposed for the FIBHM explains the formation of these pillar type structures and is more generally applicable to patterning silicon.

A high resolution TEM and electron energy loss spectrometry (EELS) analysis has been used to study the masking behaviour leading to the formation of nano-whiskers used to produce, for example, field emitters, DNA and glucose sensors, which were formed simply by an

exposure of the diamond to an oxygen plasma. **Fig. 4** examines their composition using aberration corrected Scanning TEM (STEM) and EELS mapping. Fig. 4A shows a cross-sectional image of some nano-whiskers extending vertically out of a single crystal diamond. The inset box in Fig. 4(A) (white rectangular outline) identifies the area selected for the compositional maps corresponding to background subtracted EELS signal integrals of B diamond (σ-bonded carbon), (C) iron, and (D) oxygen. The diamond is seen to form a sharp tip, but does not extend to the top of the whisker structure. Figures 4(C) and (D) show Fe and O-rich areas (respectively) forming a helmet shape over the diamond. This layer appears similar to the Fe-containing layer observed for the FIBHM and is also thicker than the penetration depth of ions in the plasma suggesting that like, $Ga^+$ FIB implanted diamond, it is again acting as a mask to the plasma etch.

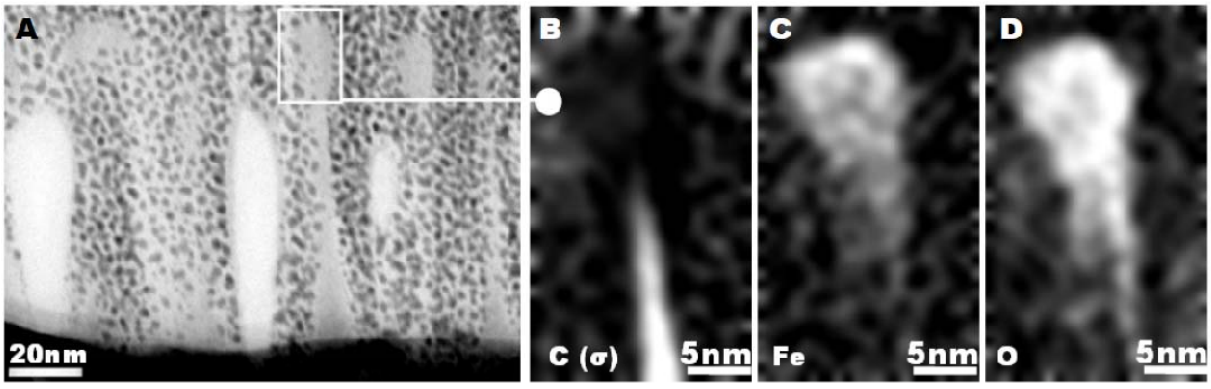


Fig. 4 (A) bright field STEM image of diamond nano-whiskers defining the areas for the EELS map for (B), (C) and (D). EELS maps corresponding to background subtracted signal integrals for; (B) σ-bonded carbon (diamond, ~35 eV), (C) iron (L edge, 710 eV) and (D) oxygen (K edge ~540 eV).

These nano-whiskers are known to originate from the presence of metal impurity, in a quantity as small as a cluster of atoms.[9] Like the "surface oxide" observed for the $Ga^+$ implanted diamond, oxides of near-surface metal impurities would have a suitably high affinity for components in the plasma to allow this iron-containing layer to deposit creating a local mask for the formation of the nano-whisker structures. Hence, we propose that these

diamond nano-whiskers form from fundamentally the same masking mechanism as that proposed for the FIBHM.

In conclusion, we propose a mechanism for the Focused Ion Beam Hard Mask (FIBHM) technique for patterning diamond, which has been demonstrated as an enabling technology for a number of technologies and presents a new form of ion beam lithography. The underlying hard mask mechanism was proposed as a surface modification induced by a FIB implantation which, on exposure to a plasma etch, leads to the formation of a non-volatile platform on which components in the plasma can deposit to subsequently protect the underlying or unmasked material from etching in the same plasma environment. We show this mechanism describes the formation of diamond nano-whiskers being used for field emitters and biosensors. We also predict that it is effective for patterning silicon and explains similar masking behavior observed in the literature.

*Experimental method*

The processing as described for the FIBHM was carried out using a focused ion beam supporting an FEI Magnum column for the ion implantation in step 1. Step 2 was performed using a South Bay Technology PC-2000 plasma etch facility. Cross-sectional TEM samples were prepared using a FIB-based ex-situ lift-out [28] technique, including a 3kV $Ga^+$ beam final polishing step, using a Carl Zeiss NVision 40 CrossBeam facility. TEM images were obtained using a JEOL 3000F field emission TEM operating at 300kV. STEM images were obtained using a custom built aberration-corrected, cold field emission VG STEM (SuperSTEM 1, SuperSTEM Laboratories, Daresbury UK) operating at 80kV. EDX analysis were performed using silicon drift detectors interfaced with; a Philips CM200 TEM operating at 200KV (results in Fig. 2), and a Hitachi s3400i SEM operating at 3kV (results in Fig. 3).

*Acknowledgements*

Authors would like to acknowledge CRANN at Trinity College Dublin where some results were obtained. In addition, the authors acknowledge financial support from the European Union under the Framework 6 program under a contract for an Integrated Infrastructure Initiative, Reference 026019 ESTEEM. We would also like to extend our appreciation for the valuable assistance at the SuperSTEM laboratories at Daresbury UK with Dr Mhairi Gass, , the University of Oxford (UK) with Dr Lisa Karlsson and Dr Gareth Hughes and the Australial Microscopy and Microanalysis Research Facility.

*References*

[1] A. D. Greentree, B. A. Fairchild, F. M. Hossain, S. Prawer, *Mater. Today* **2008**, *11*, 22.

[2] R. Kalish, *Appl. Surf. Sci.* **1997**, *117*, 558.

[3] M. P. Hiscocks, K. Ganesan, B. C. Gibson, S. T. Huntington, F. Ladouceur, S. Prawer, *Opt. Express* **2008**, *16*, 19512.

[4] C. F. Wang, R. Hanson, D. D. Awschalom, E. L. Hu, T. Feygelson, J. Yang, J. E. Butler, *Appl. Phys. Lett.* **2007**, *91*, 201112.

[5] D. S. Hwang, T. Saito, N. Fujimori, *Diam. Relat. Mater.* **2004**, *13*, 2207.

[6] G. F. Ding, H. P. Mao, Y. L. Cai, Y. H. Zhang, X. Yao, X. L. Zhao, *Diam. Relat. Mater* **2005**, *14*, 1543.

[7] H. Uetsuka, T. Yamada, S. Shikata, *Diam. Relat. Mater* **2008**, *17, 728*.

[8] J. Robertson, *Phys Status Solidi A* **2008**, *205*, 2233.

[9] E. S. Baik, Y. J. Baik, D. Jeon, *J. Mater. Res.* **2000**, *15*, 923.

[10] H. Shiomi, *Jpn. J. Appl. Phys. 1* **1997**, *36*, 4.

[11] J. Taniguchi, Y. Tokano, I. Miyamoto, M. Komuro, H. Hiroshima, *Nanotechnology* **2002**, *13*, 592.

[12] D. Luo, L. Wu, J. Zhi, *ACS Nano* **2009**, *3*, 2121.

[13] C. E. Nebel, H. Uetsuka, B. Rezek, D. Shin, N. Tokuda, T. Nakamura, *Diam. Relat. Mater* **2007**, *16*, 1648.

[14] N. Yang, H. Uetsuka, C. E. Nebel, *Diam. Relat. Mater* **2009**, *18*, 592.

[15] C. E. Nebel, N. Yang, H. Uetsuka, E. Osawa, N. Tokuda, O. Williams, *Diam. Relat. Mater* **2009**, *18*, 910.

[16] M. P. Hiscocks, C. J. Kaalund, F. Ladouceur, S. T. Huntington, B. C. Gibson, S. Trpkovski, D. Simpson, E. Ampem-Lassen, S. Prawer, J. E. Butlerc, *Diam. Relat. Mater* **2008**, *17*, 1831.

[17] E. S. Baik, Y.J. Baik, D. Jeon, *Diam. Relat. Mater* **1999**, *8*, 2169.

[18] W. McKenzie, J. Pethica, G. Cross, *Microsc. Microanal.* **2009**, *15*, 328.

[19] W. R. McKenzie, J. Pethica, G. Cross, *Diam. Relat. Mater.* **2010** (in submission).

[20] W. McKenzie, M. Hiscocks, F. Ladouceur, P. Munroe, *Microsc. Microanal.***2010**, *16*, 196.

[21] K. S. Hidenori Gamo, M. Nishitani-Gamo, T. Ando, *Jpn. J. Appl. Phys.* **2007**, *46*, 5.

[22] S. Manako, J. Fujita, Y. Ochiai, E. Nomura, S. Matsui, *Jpn. J. Appl. Phys. 2* **1997**, *36*, L724.

[23] W.R. McKenzie, M. Gass, P. Munroe, M. Quadir, *Diam. Relat. Mater.* **2010** (in submission).

[24] T. F. Yen, O. Liang, C. W. Lu, K. F. Chiu, *Microelectron. Eng.* **2007**, *84*, 1.

[25] H. X. Qian, W. Zhou, J. Miao, L. E. N. Lim, X. R. Zeng, *J. Micromech. Microeng.* **2008**, 035003.

[26] N. Chekurov, K. Grigoras, A. Peltonen, S. Franssila, I. Tittonen, *Nanotechnology* **2009**, 065307.

[27] B. Schmidt, S. Oswald, L. Bischoff, *J. Electrochem. Soc.* **2005**, *152*, G875. J

[28] M. Rogers, G. Kothleitner, A. Berendes, W. Bock, B. O. Kolbesen, *Prakt. Metallogr. Pr M* **2005**, *42*, 172.